

THE BIOMASAR ALGORITHM: AN APPROACH FOR RETRIEVAL OF FOREST GROWING STOCK VOLUME USING STACKS OF MULTI-TEMPORAL SAR DATA

Maurizio Santoro⁽¹⁾, Christian Beer⁽²⁾, Oliver Cartus⁽³⁾, Christiane Schmullius⁽³⁾, Anatoly Shvidenko⁽⁴⁾, Ian McCallum⁽⁴⁾, Urs Wegmüller⁽¹⁾, Andreas Wiesmann⁽¹⁾

⁽¹⁾ Gamma Remote Sensing AG, Worbstrasse 225, 3073 Gümligen, Switzerland,

Email: santoro@gamma-rs.ch, wegmuller@gamma-rs.ch, wiesmann@gamma-rs.ch

⁽²⁾ Max Planck Institute for Biogeochemistry, Hans Knöll Strasse 10, D-07745 Jena, Germany,

Email: cbeer@bgc-jena.mpg.de

⁽³⁾ Department of Earth Observation, Friedrich-Schiller University, Grietgasse 6, 07743 Jena, Germany,

Email: Oliver.Cartus@uni-jena.de, c.schmullius@uni-jena.de

⁽⁴⁾ International Institute for Applied Systems Analysis (IIASA), Schlossplatz 1, A-2361 Laxenburg, Austria,

Email: shvidenk@iiasa.ac.at, mcallum@iiasa.ac.at

ABSTRACT

Large-scale retrieval of forest growing stock volume (GSV) requires remote sensing techniques in order to comply with the requirements of full coverage and frequent update. With the Envisat Advanced Synthetic Aperture Radar (ASAR) instrument operating in ScanSAR mode the entire globe has been imaged since several years. ASAR's short wavelength (5.6 cm) represents a significant bottleneck for retrieving GSV because it implies weak sensitivity of the radar backscatter to forest parameters. This limitation has been partly resolved in the BIOMASAR algorithm, which combines standard image processing techniques for obtaining stacks of co-registered SAR backscatter images and an automated approach for modelling backscatter as a function of GSV, model inversion and multi-temporal combination of individual GSV estimates. For the original resolution of the SAR data (100 m and 1 km) the retrieval error is below 50%. Improved estimates with an error below 20% are obtained when aggregating GSV estimates with a factor of at least 10 (one-dimensional).

1. INTRODUCTION

Retrieval of forest growing stock volume (GSV) is a major topic of investigation in the remote sensing community due to the necessity of accurate and updated information on forest resources, which are not achievable using traditional survey methods at the regional and global level. Radar remote sensing has the advantage of being able to acquire images over any part of the Earth with a high repetition frequency. While an image can be formed regardless of cloud cover and solar illumination, the environmental conditions can play a significant role on the measurements collected by the sensor. This aspect is of particular relevance in case of forest-related studies and for high frequencies. C-band synthetic aperture radar (SAR) backscatter is generally deemed as useless when aiming at forest resources assessment due to the weak sensitivity with respect to forest parameters. Furthermore, the strong sensitivity to

the dielectric properties of the scattering objects make C-band SAR backscatter an unreliable tool for monitoring forests. Following results from a number of studies on extraction of forest parameters from SAR data, the research community tends toward a clear focus on the use of low frequency SAR.

In this paper we demonstrate that accurate estimates of forest GSV can be obtained also from C-band backscatter data under the requirement that a large stack of observations is available. The estimation of the GSV is carried out by means of the BIOMASAR algorithm, which combines conventional SAR processing techniques in the case of multi-temporal data stacks (calibration, co-registration, multi-channel speckle filter), the inversion of a Water Cloud-like model relating the GSV to the forest backscatter, and a multi-temporal combination of GSV estimates from each image. While the single parts forming the BIOMASAR algorithm approach are well documented in literature, their implementation in an automated approach to retrieve GSV is a novel aspect.

The BIOMASAR algorithm was first introduced in [1]. In this paper we present the validation of the algorithm for the boreal zone at several study areas in Sweden, Central Siberia and Québec using Envisat Advanced SAR (ASAR) ScanSAR data. The algorithm is presented in Section 2. The outcome of the validation activities concerning the modelling and the retrieval approach is described in Section 3. The accuracy assessment of GSV retrieved with the BIOMASAR algorithm is presented in Section 4. Section 5 wraps up the results and provides an outlook on future investigations.

2. BIOMASAR ALGORITHM

The BIOMASAR algorithm basically consists of two major processing steps:

- Generation of a stack of calibrated, geocoded and co-registered SAR backscatter images;

- Inversion of individual backscatter measurements by means of a Water Cloud-type of model to estimate GSV and multi-temporal combination of individual estimates of GSV.

Fig. 1 shows the block diagram of the BIOMASAR algorithm in terms of input data, additional datasets and processing sequence to retrieve GSV.

SAR processing, SAR backscatter modeling, model inversion to estimate GSV and multi-temporal combination of individual GSV estimates will be presented hereafter in related Sections. Fig. 1 shows that besides the SAR data the algorithm requires the availability of a number of additional datasets, which primarily serve to exclude pixels not representing forest land (e.g. water body, exposed rock surfaces).

2.1. SAR data processing

The aim of SAR processing is to obtain a stack of calibrated geocoded images, co-registered at sub-pixel level and with high radiometric quality, i.e. limited speckle noise. Considering the extensive number of images that need to be processed, it is preferred to use established and robust processing algorithms rather than developing area- or dataset-specific procedures, which might lead to improved image quality in single cases while the overall performance might be poorer.

The radiometric quality of the SAR images is improved by means of speckle filtering both in the spatial and in the temporal domain. Multi-looking and multi-channel filter [2] are applied. Evaluation of the Equivalent Number of Looks (ENL) after speckle filtering was ≥ 60 for both ScanSAR modes operated by Envisat (Wide Swath Mode, WSM, and Global Monitoring Mode, GMM). The corresponding residual speckle noise was below 0.6 dB.

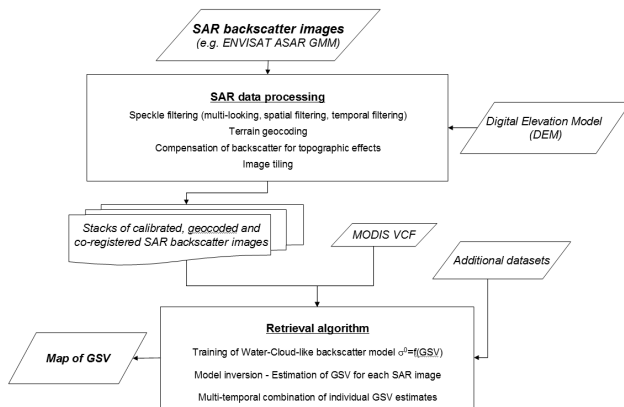


Figure 1. Flowchart of the BIOMASAR algorithm.

The main requirement for image geocoding is to obtain images that present geolocation errors of less than the pixel size. The BIOMASAR algorithm implements the automated approach described in based on cross-correlation with an image assumed to be in the correct final geometry [3, 4]. As a result of this approach, all Envisat ASAR ScanSAR data here considered were found to be co-registered at sub-pixel level. Tiling is applied to the geocoded data to obtain small stacks of co-registered images. It should be noted that multi-channel speckle filtering is applied only at this stage.

To compensate for slope-induced distortions on the backscatter, the sigma nought values are corrected for local incidence angle and effective pixel area [5]. An analysis of the GSV retrieval revealed that steep slopes facing the sensor should be masked out to avoid that topographic distortions of the backscatter affect the retrieval of GSV [6].

2.2. Backscatter modeling as a function of GSV

The retrieval of GSV from the SAR backscatter data is most robust if a physically-based model is used rather than a linear or non-linear empirical regression model. In this respect, the Water-Cloud Model with gaps [7] represents a viable solution since it has been thoroughly validated and expresses the total forest backscatter in terms of essential scattering components at C-band. In the BIOMASAR algorithm the forest backscatter is expressed as a function of GSV [8]:

$$\sigma_{for}^o = \sigma_{gr}^o e^{-\beta V} + \sigma_{veg}^o (1 - e^{-\beta V}) \quad (1)$$

In Eq. (1) σ_{for}^o represents the forest backscatter and V the growing stock volume. The model includes three parameters that are unknown *a priori*: the backscatter coefficient of the forest floor, σ_{gr}^o , the backscatter coefficient of the vegetation layer, σ_{veg}^o , and an empirically defined coefficient expressed in ha/m^3 , β , related to the forest transmissivity, $e^{-\beta V}$. Typically, the estimation of the three model parameters is carried out by means of least-squares regression using a dataset of reference forest GSV measurements and corresponding backscatter observations. This approach is however unfeasible when aiming at covering large areas because it would imply having a dense network of training sites to capture possible spatial variations of the SAR backscatter due to heterogeneous forest structure or environmental conditions. In this paper we overcome this shortcoming with an approach for model training that does not rely on *in situ* measurements. It will be hereafter assumed that the estimation and the retrieval are described at the pixel level.

The parameter σ_{gr}^o represents the backscatter in case of an unvegetated surface. Hence, it can be assumed that a reasonable estimate corresponds to a central statistics

measure of the backscatter for pixels that can be labeled as unvegetated within a window of finite size centered in the pixel of interest. These pixels will be referred to as “ground” pixels. Similarly, an estimate of the parameter σ_{veg}^0 can be obtained from a measurement of central tendency of the backscatter of dense forest within a similar window. Rigorously speaking, σ_{veg}^0 represents the backscatter in the case of a completely opaque forest canopy. Because of gaps, even in the densest forest, a fraction of the measured backscatter is represented by the ground contribution. Hence, in order to obtain an estimate for σ_{veg}^0 , compensation of the measured backscatter over dense forests for the residual backscatter component from the ground is necessary. Since σ_{gr}^0 is known at this stage, Eq. (1) can be inverted to obtain σ_{veg}^0 from the backscatter of the pixels forming a so-called “dense forest” class.

$$\sigma_{veg}^0 = \frac{\sigma_{df}^0 - \sigma_{gr}^0 e^{-\beta V_{df}}}{1 - e^{-\beta V_{df}}} \quad (2)$$

In Eq. (2) σ_{df}^0 represents the backscatter in the “dense forest” class. The estimation of σ_{veg}^0 requires knowledge of the parameters β and V_{df} , the latter representing a GSV value representative for the “dense forest” class.

In case of low resolution data, the estimation of the parameters σ_{gr}^0 and σ_{df}^0 can profit from the use of continuous tree canopy cover products based on optical remote sensing such as the MODIS Vegetation Continuous Fields (VCF) tree cover product. The MODIS VCF product represents continuous estimates of percentages of tree cover with a 500 m pixel size [9], thus being a well-suited image product for automatic selection of SAR backscatter values belonging to the “ground” and the “dense forest” class. It is here remarked that the VCF product is used solely as mask to select pixels to be labeled as “ground” and “dense forest”; the actual values of tree cover percentage are not used by the BIOMASAR algorithm.

The parameter β is in theory related to dielectric properties of the vegetation (e.g. frozen/unfrozen conditions) and forest structural properties. Previous investigations [10] as well as an analysis of the VCF parametrized as a function of GSV [10] showed that this parameter can vary but no consistent behavior was found in terms of seasonal conditions or forest type. As a trade-off between computational efficiency and retrieval performance, it was decided to set β equal to 0.006 ha/m^3 . This assumption takes into account the fact that fine tuning of the model parameter to local environmental conditions and forest type characteristics is unrealistic due to the paucity, if not lack, of large-scale detailed information on weather conditions and forest structural properties.

The GSV value for the “dense forest” class, V_{df} , represents a fictitious GSV level that can be assumed to characterize the densest forests within the area to which the pixel belongs to. The definition of this parameter requires some *a priori* knowledge on the spatial distribution of GSV at the area of interest. Information on the distribution of GSV is generally available at regional level from average statistics of GSV available in national and regional inventory data. Attaching one value of V_{df} to an area of the size of a region, i.e. of several thousands of km^2 , is reasonable considering that spatial variations of the GSV for the densest forests are small at kilometric resolution.

2.3. Retrieval of GSV

Once the model parameters have been estimated, the model in Eq. (1) can be inverted to derive an estimate of GSV from a measurement of the SAR backscatter.

$$\hat{V} = -\frac{1}{\beta} \ln \left(\frac{\sigma_{veg}^0 - \sigma_{for}^0}{\sigma_{veg}^0 - \sigma_{gr}^0} \right) \quad (3)$$

In Eq. (3) \hat{V} represents the retrieved GSV in correspondence of the backscatter measurement, σ_{for}^0 . At C-band, it is likely that the SAR backscatter is not within the range of modeled backscatter values, especially in the case of high GSV because of the reduced sensitivity of the backscatter. This issue requires the modeling and the inversion to be constrained to a certain range of backscatter values and GSV. The rules for the retrieval are illustrated in Fig. 2.

The backscatter is modeled up to a certain GSV, referred to as maximum retrievable GSV (e.g. $300 \text{ m}^3/\text{ha}$). This represents the highest level of GSV typically found in the area of interest; this information is generally available from coarse-scale inventory data. If a backscatter measurement is not within the range of modeled values but close enough to it (buffer zone), the retrieved GSV is set equal to 0 or the maximum retrievable GSV depending whether it is closer to the modeled value for the former or the latter GSV value. The width of the buffer zone is set equal to the magnitude of residual speckle noise. Otherwise the retrieved GSV is set to not-a-number (outlier zone).

To decrease the amount of noise in individual GSV estimates, a weighted combination is used:

$$\hat{V}_{mt} = \frac{\sum_{i=1}^N \frac{w_i}{w_{\max}} \hat{V}_i}{\sum_{i=1}^N \frac{w_i}{w_{\max}}} \quad (4)$$

In Eq. (4) \hat{V}_i represents the *i*-th estimate of GSV and $w_i = (\sigma_{veg}^0 - \sigma_{gr}^0)_i$ is the corresponding weight based on the

difference between the two model parameters representing the backscatter of vegetation and ground. It is assumed that backscatter measurements characterized by stronger sensitivity of the backscatter to GSV should weight more in the multi-temporal combination. N is the number of measurements for which an estimate of GSV has been obtained. The coefficient w_{max} corresponds to the largest of the w_i weights.

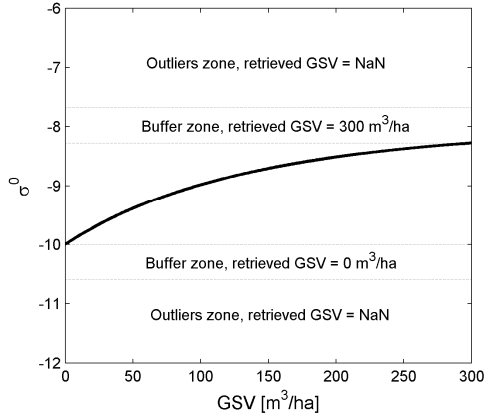


Figure 2. Modeled backscatter as a function of GSV and definition of retrieval rules.

3. ALGORITHM VALIDATION

The validation of the BIOMASAR algorithm aimed at confirming the plausibility of the approaches used to estimate the model parameters and to retrieve GSV. For this scope datasets of reference GSV measurements (from *in situ* or remotely sensed data) were gathered for each study area. Another objective of the investigations was to prove the robustness of the retrieval algorithm with respect to the temporal and spatial variability of the backscatter.

3.1. Estimation of σ_{gr}^0

The estimation of the parameter σ_{gr}^0 requires the definition of a window of finite size, centered in the pixel of interest, in which pixels corresponding to a low value of the MODIS VCF product are selected. A measure of central tendency for the distribution of the so-called “ground” pixels is then used to determine the model parameter estimate. To account for skewness due to spatial variability of the backscatter, the median is used since it proved to be the most reliable measure of the central tendency.

The robustness of the procedure for estimating σ_{gr}^0 was tested by checking the sensitivity of the estimates to window size and an upper threshold on VCF and compare to the estimate obtained using the traditional approach based on least-squares regression between measurements of GSV and backscatter [10]. Since the number of “ground” pixels in an estimation window

depends on both the size of the window and on the VCF threshold, a sensitivity analysis could not be performed without considering the two aspect simultaneously. The sensitivity analysis was carried out by computing a value of σ_{gr}^0 for a set of combinations of VCF threshold and window size. The VCF threshold was varied between 15 and 25%. The radius of the estimation window was varied between 50 and 200 pixels. With smaller thresholds and/or radius hardly ever more than a few pixels could be selected as “ground”. The highest VCF threshold was limited to 25% to avoid that vegetation might affect the backscatter distribution significantly. VCF of 30-40% generally corresponds to shrubland in global land-cover datasets. A radius of the estimation window larger than 200 pixels did not affect the estimation of σ_{gr}^0 .

When more than 2% of the pixels were selected as “ground” pixels, the estimates of σ_{gr}^0 agreed with the values obtained using the traditional model training approach. Satisfactory results were obtained with a 1% limit. Large discrepancies were observed for very small datasets of “ground pixels”. When furthermore comparing the percentage of “ground” pixels in the estimation window with the outcome of an analysis of the backscatter distribution by means of the Hartigan’s dip test on unimodality [11] it could be observed that (i) for a percentage of “ground” pixels below 1% the dip test always stated the lack of unimodality and (ii) for at least 2% “ground” pixels, the dip test always stated unimodality. Based on such results the estimation procedure was set up as described in the flowchart in Fig. 3.

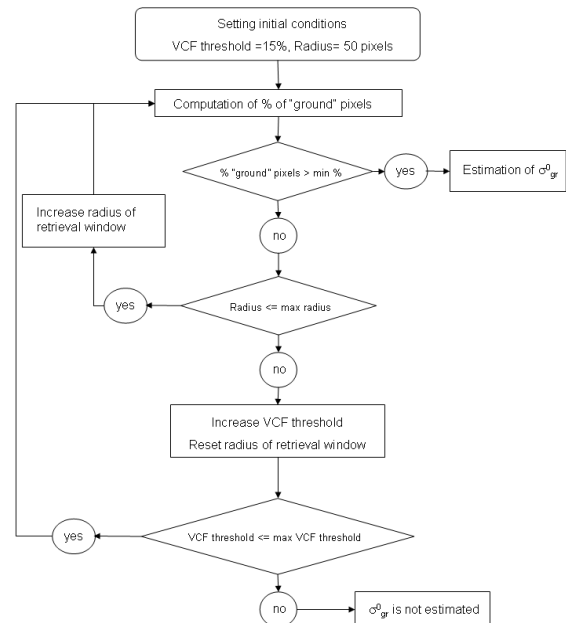


Figure 3. Estimation of the model parameter σ_{gr}^0 in the BIOMASAR algorithm.

Starting from a initial condition on window size and VCF threshold, the window size and, in second instance, the VCF threshold are increased until at least 2% of the pixels within the window are labeled as “ground”. Fall back on a 1% level is considered in case the percentage of pixels selected as “ground” is always below 2%. If the percentage of the “ground” pixels never reaches the 1% level, σ_{gr}^0 is set equal to not-a-number, which in turn means that no GSV will be retrieved for the specific backscatter measurement.

3.2. Estimation of σ_{veg}^0

The estimation of the parameter σ_{veg}^0 also relies on the definition of an estimation window and selection of pixels that in this case will belong to a “dense forest” class. These correspond to pixels showing a VCF value above a certain threshold. To obtain σ_{veg}^0 , the central tendency of the backscatter for dense forests, σ_{df}^0 , needs to be corrected for residual contribution from the forest floor as shown in Eq. (2). Therefore, a sensitivity analysis aiming at defining rules for a robust estimation of σ_{veg}^0 had to consider (i) the sensitivity of σ_{df}^0 to the size of the estimation window and VCF threshold, i.e. in terms of the percentage of “dense forest” pixels within the window, and (ii) the sensitivity of σ_{veg}^0 to the GSV for dense forests, V_{df} . In principle, the sensitivity analyses should have also considered the propagation of estimation errors of σ_{gr}^0 and/or β . This aspect was however considered of minor importance since the compensation of the backscatter from dense forests to obtain the estimate of σ_{veg}^0 should be minimal at C-band.

The VCF threshold was constrained between 70 and 80% of the maximum VCF value in order to include only dense forests in the “dense forest” class and capture at least 2% of “dense forest” pixels. The radius of the window was allowed between 50 and 100 pixels in order to include at least 2% of pixels. Larger estimation windows always included more than 2% of “dense forest” pixels and the estimates did not differ compared to the case of 100 pixels. For the GSV of dense forest, values between the 80th and the 95th percentile of the GSV histograms from the reference data were considered. The percentage of dense forest pixels was found to be generally high enough to obtain clearly peaked backscatter distribution. The measure of central tendency used to estimate σ_{df}^0 did not play a significant role on the performance of the algorithm.

All combinations were found to provide an estimate of σ_{veg}^0 for which the model in Eq. (1) describes the trend between the backscatter measurements and the reference GSV values. Nonetheless, some model realizations were closer to the average backscatter trend in a least squares sense than others. To gain insight on the estimation sensitivity, the mean difference of the backscatter

measurements with respect to the specific model realization, MD, was computed:

$$MD = \sqrt{\frac{1}{N} \sum_{i=1}^N (\sigma_{meas,i}^0(V_i) - \sigma_{model,i}^0(V_i))^2} \quad (5)$$

where $\sigma_{meas,i}^0$ and $\sigma_{model,i}^0$ represent the measured and the modeled backscatter respectively, and V_i represents the GSV for the i -th pixel. Since the focus is on dense forests, MD was computed for pixels with GSV above 70% of the maximum GSV in the area of investigation (i.e. > 150-200 m³/ha). Hence, N represents the number of reference pixels in the estimation window satisfying this requirement. For each combination of (i) VCF threshold for dense forest, (ii) estimation window size and (iii) GSV for dense forest, the statistics of MD across the stack of data were analyzed. Combinations for which the predicted value of σ_{veg}^0 corresponded to a model realization closer to the trend in the observations were characterized by three criteria: i) small average MD, ii) small standard deviation of MD and iii) limited span of MD values.

The only consistent trend at the study areas was a low average MD with small dispersion for a combination of (i) estimation window with a radius of 100 pixels, (ii) minimum VCF for dense forest of 75% of the maximum value and (iii) GSV for dense forest equal to the 90th percentile of the GSV distribution for the area being investigated. Settings (i) and (ii) could be easily implemented in the algorithm. Concerning the GSV of dense forests, the sensitivity analysis revealed weak impact of the actual value, i.e. the definition of V_{df} does not require exact knowledge of the distribution of GSV for the area of interest. For simplicity, in the BIOMASAR algorithm, V_{df} is set equal to the maximum GSV for the area of interest, i.e. a value commonly reported in forest inventory statistics.

3.3. Modelled backscatter with the BIOMASAR algorithm

Forest backscatter modeling is applied to each pixel and for each image in order to cope with spatial and temporal variations of the backscatter. The output of the model training block consists of images of σ_{gr}^0 and σ_{veg}^0 for each acquisition date. Fig. 4 shows an example of modeled and measured backscatter representative for the study areas at which the algorithm validation was carried out. The upper plot shows the measurement of backscatter for a pixel (filled circle) with respect to the *in situ* GSV, the model realization for the pixel using σ_{gr}^0 and σ_{veg}^0 estimated by the BIOMASAR algorithm (solid curve) and the trend of the backscatter measurements as a function of inventory GSV for the area surrounding the pixel of interest. The modeled backscatter followed the trend of the measurements. The histograms at the bottom show the distribution of the

backscatter for “ground” pixels (left) and “dense forest” pixels (right) respectively for the window size/VCF threshold selected by the algorithm and reported on top of each plot. The percentage of “ground” pixels was rather small; however, still a plausible estimate of σ_{gr}^0 was obtained (asterisk in the upper plot at 0 m³/ha). The median-based estimation performed well, representing the central tendency of the distribution. The histogram for the “dense forest” class presented a slightly skewed form (bottom right plot). The estimate of σ_{df}^0 through the median was however only minimally shifted with respect to the peak of the histogram.

The agreement between measured and modeled backscatter was in general high. Only in a few cases the model realization did not reflect the backscatter at the lowest GSV, which is however to be considered physiological when looking at several hundred backscatter observations per pixel. In such cases the modeled backscatter was mostly insensitive to GSV, whereas the measurements showed an increase of backscatter with GSV. Taking into consideration that the multi-temporal combination has been implemented in order to reject GSV estimates with a very small contrast between unvegetated and densely forested areas, see Eq. (4), erroneous estimates of the model parameters did not affect the retrieval of GSV.

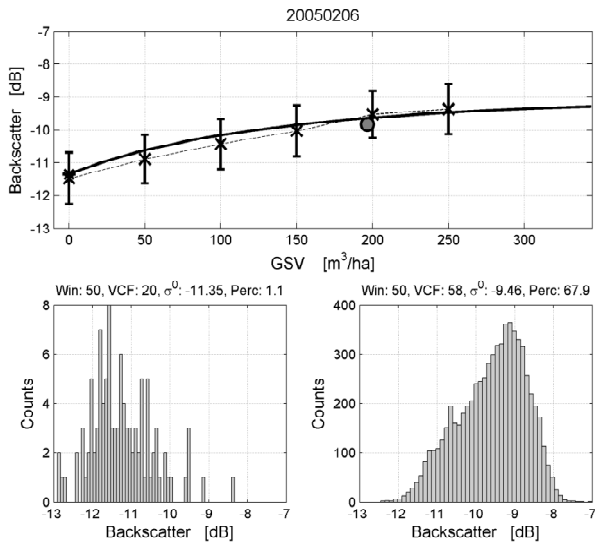


Figure 4. Performance analysis of backscatter modeling with the BIOMASAR algorithm. For details it is referred to the text.

3.4. Estimation of GSV from a single measurement

The only factor that plays a significant role on the performance of the model inversion is the maximum retrievable GSV. Because of the reduced sensitivity of the C-band backscatter at high GSV, an increase or decrease of the level of the maximum retrievable GSV implies increase or decrease of the retrieved GSV for a

number of observations, which in turn affects the multi-temporal estimate of GSV in the form of an offset. To assess the sensitivity of the retrieval to the level of maximum retrievable GSV, the GSV was retrieved with the BIOMASAR algorithm using each time a different level for the maximum GSV and then aggregated at the level of a study area. The average GSVs were then compared against the average GSV value obtained from the reference data. Use of aggregated values was preferred to avoid that pixel-wise noise and errors might influence the analysis. For increasing level of maximum GSV the aggregated GSV predicted by BIOMASAR increased linearly. The best agreement was obtained when an offset of 40-50 m³/ha was added to V_{df} . For this reason it has been decided to define the maximum retrievable GSV, V_{max} , simply as:

$$V_{max} = V_{df} + 50 \quad (6)$$

3.5. Multi-temporal retrieval of GSV

The use of the backscatter difference ($\sigma_{veg}^0 - \sigma_{gr}^0$) as weight proved to be plausible when plotting individual GSV estimates (dots and circles) against the corresponding weight for the multi-temporal combination, w_i (Fig. 5). The GSV estimated from observations characterized by large weights, i.e. strong sensitivity to the backscatter, are closer to the reference value shown by the horizontal line. In addition, the multi-temporal GSV is in line with the reference value. The multi-temporal combination implemented in the BIOMASAR algorithm discards GSV estimates characterized by low or negative weights to avoid the effect of substantial errors contained in GSV estimates in consequence of strong environmental conditions effect or incorrect modelling. The 0.5 dB level was found to represent a reasonable compromise between keeping a large number of observations and guaranteeing that incorrect GSV estimates are discarded.

Fig. 5 also gives insight on the effect of the seasonal conditions on the retrieval. The larger weights and the stronger agreement between the retrieved and the reference GSV was often obtained for frozen ($T < -3^\circ C$) conditions. Increased penetration of the microwave into the forest canopy, implied scattering from larger elements of the trees. Unfrozen conditions ($T > 5^\circ C$) were characterized by lower weights and larger discrepancies between the retrieved and the reference GSV, as a consequence of the sensitivity to wet/dry environmental conditions. Under freeze/thaw conditions ($-3^\circ \leq T \leq 5^\circ C$) the estimation was rather unpredictable. The measured backscatter in such cases is strongly affected by external factors such as snow wetness and structure. Fig. 5 shows that the sensitivity of the backscatter to GSV was mostly between 2 and 4 dB for frozen conditions, up to 3 dB for unfrozen conditions and mostly below 2 dB for freeze/thaw conditions.

Increasing the minimum weight, i.e. reducing the multi-temporal combination to cases presenting the largest forest backscatter variability, did not perform better than when the 0.5 dB level was considered. This was proved by sorting images for increasing average weight and adding each time to the multi-temporal dataset one observation. The relative RMSE for the multi-temporal combination decreased significantly when combining the first few images with the largest weights. The retrieval continued improving even if marginally when further including estimates corresponding to an observations characterized by smaller average weights as shown in Fig. 6.

The investigations indicated that at least 20 estimates of GSV, i.e. backscatter measurements, satisfying the criterion of a weight above 0.5 dB are necessary for a substantial improvement of the final GSV estimate with respect to individual GSV estimates. It is however difficult to define the amount of backscatter observations needed to start with, since environmental conditions play a significant role on the backscatter sensitivity to GSV. Starting with 60-100 backscatter measurements seemed sufficient to reach the mass of data required for optimal performance, under the assumption that repeated acquisitions have been collected during all seasons. Selection of GSV estimates to be used for the multi-temporal combination requires simply that the corresponding weight is above the 0.5 dB threshold, regardless of environmental conditions.

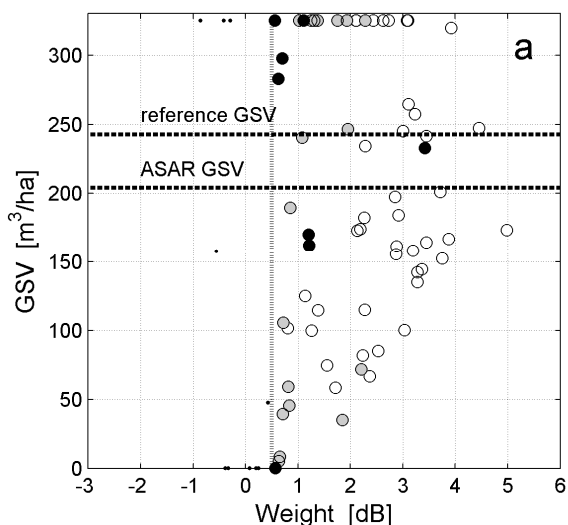


Figure 5. Retrieved GSV as a function of the weight w_i for a pixel with $GSV=246 \text{ m}^3/\text{ha}$. Each point represents a GSV estimate. Dots indicate GSV estimates discarded from the multi-temporal combination. Circles indicate GSV estimates accepted for the multi-temporal combination. Different shadings have been used to identify the environmental conditions at the time of image acquisition (white-fill=frozen, grey-fill=unfrozen, black-fill=freeze/thaw).

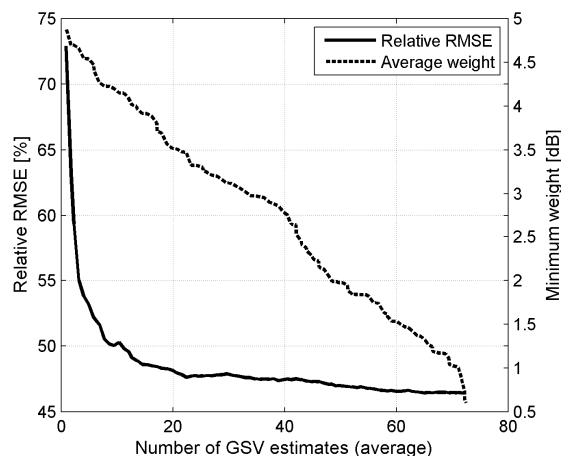


Figure 6. Relative RMSE and minimum weight with respect to average number of GSV estimates, i.e. observations, selected for the multi-temporal combination.

4. VALIDATION OF FOREST GSV RETRIEVAL

The validation of the GSV retrieval consisted of a comparison of the multi-temporal GSV against the GSV from the reference datasets. For the Siberian and the Swedish study areas, dense datasets of WSM and GMM images with a pixel size of respectively 100 m and 1 km were available, which allowed an assessment of the impact of spatial resolution of the GSV estimates on the retrieval. The results were similar; however, local errors in the reference data at the 100 m scale affected the retrieval statistics for the WSM data.

The availability of both ScanSAR data types also allowed investigating whether increasing the number of observations at lower resolution by multi-looking the WSM data lead to an improved retrieval. Populating the GMM dataset with aggregated WSM observations slightly increased the retrieval accuracy with respect to a retrieval based on only one of the two modes. Combining the two datasets has the advantage that a dense dataset can be achieved over a short period of time (e.g. one year), thus preventing the retrieval from being affected by forest cover changes. Hereafter, we will focus on the results obtained at 1 km from a combined GMM-WSM dataset.

The relative RMSE was between 34.2% and 48.1%. The different results were primarily related to the quality of the data available at the study areas that could be used for reference. Fig. 7 shows the retrieved and the reference (inventory) GSV for the study area in Central Siberia for which a relative RMSE of 34.2% was obtained. The plot shows reasonable agreement between the two datasets, without apparent sign of saturation up to $300 \text{ m}^3/\text{ha}$, which is well beyond the expected capability of C-band backscatter to retrieve forest GSV.

For GSV greater than $300 \text{ m}^3/\text{ha}$ the scatterplot seems to indicate saturation. The pattern shown in Fig. 7 was observed at the other study areas as well, although there the GSV did not reach $300 \text{ m}^3/\text{ha}$. The scatterplot shows significant spread, which could be ascribed to the weak sensitivity of C-band backscatter to forest structural parameters as well as to local errors in the reference dataset. The uncertainty of the retrieval due to the algorithm was assessed by perturbing each of the parameters discussed in Section 3. The effect was limited; the mean value of the uncertainty was 9.6% with a standard deviation of 3.2%.

To verify to which extent the noise and uncertainty affect the ASAR and the in situ datasets, aggregation of GSV estimates was applied. Fig. 8 illustrates the trend of the correlation coefficient between retrieved and reference GSV and the relative RMSE as a function of aggregated pixel size. The agreement between the retrieved and the reference GSV increased with increasing aggregation level, in particular when the aggregation factor was small (approximately 5×5). For larger aggregation levels the increase in correlation was marginal. The same pattern was for WSM data at the starting from the original pixel size, i.e. 100 m.

Fig. 9 shows the scatterplot between the aggregated values from the retrieved and the reference GSV datasets for 10 km pixel size, for the study area in Central Siberia. The agreement is remarkable, without apparent signs of saturation for the entire range of GSV, i.e. $0\text{--}300 \text{ m}^3/\text{ha}$. Similar patterns have been obtained at the other study areas as well. This proves that aggregation reduced noise substantially, thus showing the effective potential of the retrieval approach implemented in the BIOMASAR algorithm when applied to C-band backscatter data.

5. CONCLUSIONS

In this paper we have presented the validation of an algorithm for retrieval of forest GSV using hyper-temporal stacks of SAR backscatter measurements. The algorithm has been successfully validated with Envisat ASAR ScanSAR data at different study areas in the boreal zone. The retrieval relative RMSE was generally below 50% for full resolution data (100 m and 1 km) and below 20% for aggregated versions at reduced spatial resolution (at least factor 10, one-dimensional). The most prominent result is that the estimates of GSV were in line with reference data practically for the entire range of GSV found at the study areas. This result opens up the possibility for exploiting the extensive archives of ENVISAT ASAR ScanSAR data for pan-boreal forest GSV retrieval at a spatial resolution required by process-based biosphere and carbon accounting models, and at an annual basis contributing to the assessment of carbon emissions by disturbances and wood harvest.

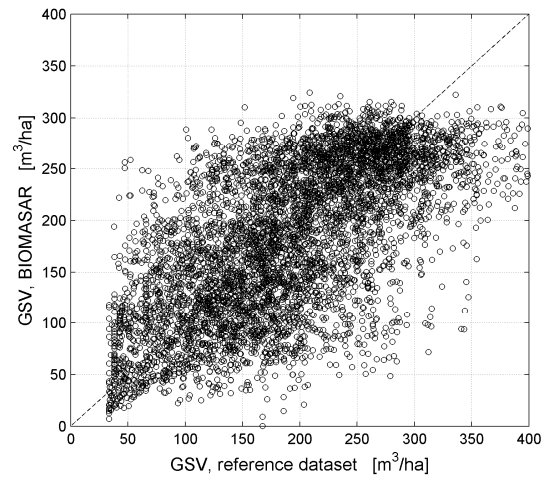


Figure 7. Scatterplot of retrieved vs. in situ GSV at 1-km spatial resolution for a study area in Central Siberia. Relative RMSE: 34.2%; estimation bias: $-8.3 \text{ m}^3/\text{ha}$; correlation coefficient: 0.65.

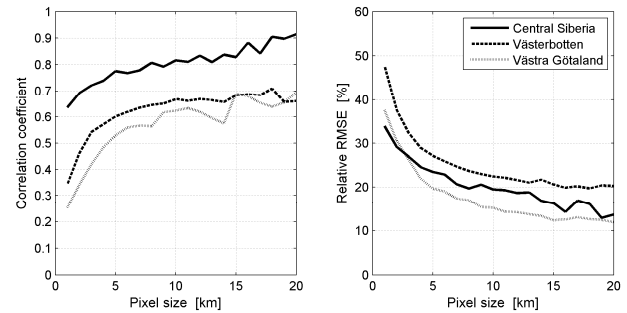


Figure 8. Correlation coefficient (left) and relative RMSE (right) as a function of aggregation level expressed in terms of pixel size of the aggregated GSV estimates for three study areas.

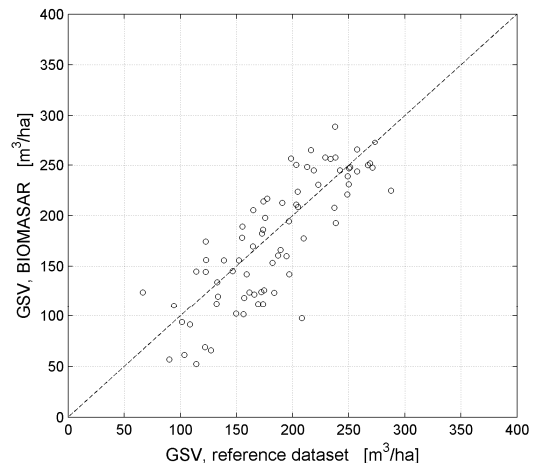


Figure 9. Scatterplot of retrieved vs. in situ GSV for the study area in Central Siberia at 10-km pixel size. Relative RMSE: 19.7%; estimation bias: $-7.0 \text{ m}^3/\text{ha}$; correlation coefficient: 0.82.

ACKNOWLEDGEMENTS

This study was supported by ESA's Support to Science Element (STSE) BIOMASAR Project. Envisat ASAR data was obtained through ESA's AO-225 and Category-1 project nr. 6397. J. Fransson and M. Nilsson, SLU, A. Beaudoin, LFC, are acknowledged for provision of reference GSV data. Collection of in situ data in Siberia was supported by the EC-funded Projects SIBERIA and SIBERIA-II. Weather data was obtained from DWD.

REFERENCES

1. Santoro, M., Beer, C., Shvidenko, A., McCallum, I., Wegmüller, U., Wiesmann, A. & Schmullius, C. (2007). Comparison of forest biomass estimates in Siberia using spaceborne SAR, inventory-based information and the LPJ Dynamic Global Vegetation Model. In *Proc. Envisat Symposium 2007* (Ed. H. Lacoste), ESA SP-636 (CD-ROM), ESA Publications Divisione, European Space Agency, Noordwijk, The Netherlands.
2. Quegan, S. & Yu, J.J. (2001). Filtering of multichannel SAR images. *IEEE Trans. Geosci. Remote Sensing*. **39**(11), 2373-2379.
3. Wegmüller, U. (1999). Automated terrain corrected SAR geocoding. In *Proc. IGARSS'99*, IEEE Publications, Piscataway, NJ, pp1712-1714.
4. Wegmüller, U., Werner, C., Strozzi, T. & Wiesmann, A. (2002). Automated and precise image registration procedures. In: *Analysis of Multi-temporal remote sensing images* (Eds. Bruzzone & Smits), World Scientific, 37-49.
5. Wiesmann, A., Wegmüller, U., Santoro, M., Strozzi, T. & Werner, C. (2004). Multi-temporal and multi-incidence angle ASAR Wide Swath data for land cover information. In *Proc. 4th International Symposium on Retrieval of Bio- and Geophysical Parameters from SAR Data for Land Applications*, CD-ROM.
6. Santoro, M. & Cartus, O. (2010). STSE-BIOMASAR: Validating a novel biomass retrieval algorithm based on hyper-temporal Wide-Swath and Global Monitoring Envisat ASAR datasets. Final Report.
7. Askne, J., Dammert, P.B.G., Ulander, L.M.H. & Smith, G. (1997). C-band repeat-pass interferometric SAR observations of the forest. *IEEE Trans. Geosci. Remote Sensing*. **35**(1), 25-35.
8. Pulliainen, J.T., Heiska, K., Hyypä, J. & Hallikainen, M.T. (1994). Backscattering properties of boreal forests at the C- and X-bands. *IEEE Trans. Geosci. Remote Sensing*. **32**(5), 1041-1050.
9. Hansen, M.C., De Fries, R.S., Townshend, J.R.G., Carroll, M., Dimiceli, C. & Sohlberg, R.A. (2003). Global percent tree cover at a spatial resolution of 500 meters: first results of the MODIS Vegetation Continuous Field algorithm. *Earth Interactions*. **7**(10), 1-15.
10. Santoro, M., Askne, J., Smith, G. & Fransson, J.E.S. (2002). Stem volume retrieval in boreal forests from ERS-1/2 interferometry. *Remote Sens. Environ.* **81**(1), 19-35.
11. Hartigan, J.A. & Hartigan, P.M. (1985). The dip test of unimodality. *Annals of Statistics*. **13**, 70-84.